

## Deformed-jellium model for the fission of multiply charged simple metal clusters

F. Garcias

*Departament de Física, Universitat de les Illes Balears, E-07071 Palma de Mallorca, Spain*

A. Mañanes

*Departamento de Física Moderna, Universidad de Cantabria, E-39005 Santander, Spain*

J. M. López and J. A. Alonso

*Departamento de Física Teórica, Universidad de Valladolid, E-47011 Valladolid, Spain*

M. Barranco

*Departament d'Estructura i Constituents de la Matèria, Facultat de Física, Universitat de Barcelona, Diagonal-647, E-08028 Barcelona, Spain*

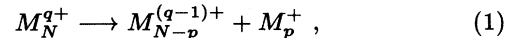
(Received 25 August 1994)

A deformed-jellium model is used to calculate the fission barrier height of positive doubly charged sodium clusters within an extended Thomas-Fermi approximation. The fissioning cluster is continuously deformed from the parent configuration until it splits into two fragments. Although the shape of the fission barrier obviously depends on the parametrization of the fission path, we have found that remarkably, the maximum of the barrier corresponds to a configuration in which the emerging fragments are already formed and rather well apart. The implication of this finding in the calculation of critical numbers for fission is illustrated in the case of multiply charged Na clusters.

The electrostatic repulsion in isolated positive multiply charged metal clusters may lead them to dissociate into aggregates with smaller sizes and charges.<sup>1</sup> As a consequence of this phenomenon, multiply charged metal clusters  $M_N^{q+}$  are usually observed in mass spectra only if the number  $N$  of atoms exceeds a critical size  $N_c$  that depends on the metal species  $M$  and on the charge state  $q$ . The critical numbers for multiply charged alkali-metal clusters up to  $q = 7$  have been recently determined.<sup>2,3</sup> The existence of these critical values can be explained by the competition between two main fragmentation mechanisms for excited multiply charged clusters,<sup>4</sup> evaporation of a neutral monomer and fission into two charged fragments, with preferential emission of fragments with a "magic" number of electrons (such as  $\text{Li}_3^+$ ,  $\text{Na}_3^+$ ,  $\text{K}_3^+$ , or  $\text{K}_9^+$ ) (Ref. 5) due to electronic shell effects. Hot large clusters lose their excitation energy mainly evaporating neutral atoms, whereas for small clusters the preferred decay channel is asymmetric fission. Both fragmentation processes compete for cluster sizes around  $N_c$ , and under certain experimental conditions some  $M_N^{q+}$  clusters have also been detected below  $N_c$ .<sup>6</sup>

Old theoretical studies of cluster stability were based on pure energetic criteria which only involved the energies of the initial and final states.<sup>7-9</sup> But the experimental findings indicate that cluster fission is a barrier-controlled process, and have prompted the interest of theoreticians to obtain these barriers.<sup>10-16</sup> For large clusters monomer evaporation is favored over fission because the barrier against fission is larger than the heat of evaporation of the monomer. On the other hand, small clusters may undergo fission because the barrier height is, in this case, smaller than the heat of evaporation. Consequently,

a fundamental understanding of the critical number  $N_c$  requires the calculation of the fission barrier for the process



and the same can be said for  $N_c^*$ , the critical number for spontaneous fission ( $N_c^*$  is the size for which the fission barrier becomes zero; it is smaller than  $N_c$ ).

Microscopic descriptions of the dynamics of the fission process, based on local spin-density functional calculations for the electronic structure in conjunction with molecular dynamics simulations, have been performed for small doubly charged alkali-metal clusters.<sup>16</sup> These calculations clearly show the influence of electronic shell effects on the fission energetics and barriers heights (predominance of an asymmetric fission channel, double-hump fission-barrier shapes, etc). Whether or not these results can be generalized to large systems is difficult to ascertain, since microscopic calculations are not feasible for large multiply charged clusters. A systematic investigation of fragmentation processes for clusters as large as  $\text{Na}_{445}^{7+}$  (Refs. 2 and 3) calls at present for much simpler, yet reliable methods to tackle the problem. One of the simplest methods is the liquid drop model, in which the metallic character of the fissioning system is taken into account by explicitly concentrating the net charge on the cluster surface.<sup>12</sup> Shell effects have been included in this model by applying the shell correction method of Strutinsky (originally developed in nuclear physics<sup>17</sup>) to study symmetric<sup>14</sup> and asymmetric fission of doubly charged silver clusters<sup>18</sup> and of highly charged alkali-metal clusters.<sup>3</sup> However, this type of calculation misses

the sizable spillout of the electronic distribution beyond the cluster edge.

The aim of the present work is to address the study of the fragmentation of multiply charged simple metal clusters within a different approach, namely, the density functional theory<sup>19</sup> using a self-consistent deformed-jellium (DJ) model. One of the merits of this model is that the electronic spillout is self-consistently treated. Previous work<sup>15,20–22</sup> lies on the assumption that the fragments are already preformed at the early stages of the fission process, that is, before surpassing the barrier maximum. This means that to obtain the fission barrier height  $F_m$  one starts with a cluster of  $N - q$  valence electrons moving in the mean field created by two tangent jellium pieces with  $N - p$  and  $p$  atoms, respectively, and the cluster fragmentation path is obtained by increasing the distance between those two jellium pieces, which were taken as spheres. We then get  $F_m$  as the difference between the energy at the maximum of the barrier and that of the spherical parent cluster  $M_N^{q+}$ . Here, we shall substantiate the above crucial assumption of the two-jellium-sphere (TJS) model and, consequently, offer a sound and easy way to calculate the fission-barrier height for simple metal clusters of (almost) arbitrarily large size and charge state.

For this purpose we have described the fission path by a series of deformed-jellium shapes connecting the initial configuration of the parent cluster with the final one corresponding to two separated fragments. More precisely, the positive background of the fissioning cluster is modeled by axially symmetric jellium shapes corresponding to two spheres smoothly joined by a portion of a third quadratic surface of revolution.<sup>23</sup> This family of shapes is characterized by the values of three parameters: the asymmetry  $\Delta$ , the distance parameter  $\rho$  which is proportional to the separation  $s$  between the emerging fragments, and the “deck” parameter  $\lambda$  which takes into account the neck deformation. In this DJ model, the jellium self-energy and the jellium potential acting on the electrons, which are both analytical functions in the TJS model, have to be calculated numerically (see Ref. 24 for details). Given a cluster configuration defined by a set of values of the jellium parameters  $(\Delta, \rho, \lambda)$ , the density of the valence electrons is self-consistently calculated by minimizing the total energy of the system for this fixed jellium background configuration. To obtain the barrier corresponding to a fission channel we compare the results following different fragmentation pathways, defined by the relations between the parameters  $\lambda$  and  $\rho$  ( $\Delta$  is fixed by the size of the final fragments). As a general criterion we start with a sphere ( $\lambda = 1 - \Delta, \rho = \Delta$ ) and follow the line corresponding to a cone capped with spheres ( $\lambda = 1 - \Delta^2/\rho$ ) up to a configuration where the neck starts to form. Next, we have chosen the line of fastest variation of the neck, which corresponds to the relation  $(\lambda - 1)^2 - \rho^2 = \text{const}$ , up to  $\lambda = 0$ . From the theoretical results of Ref. 16 this fission path seems to be the one giving the minimum barrier height (see Figs. 2 and 4 below). Anyway, other parametrizations leading to cluster shapes much more compact (Fig. 1) or elongated (Fig. 3) will be compared.

As a first application of the DJ model, we have carried out some extended Thomas-Fermi (ETF) calculations for the symmetric fission of  $\text{Na}_{42}^{2+}$  using the energy density functional of Ref. 20. Due to shell effects, symmetric fission is predicted to be the preferred fragmentation channel for this cluster.<sup>21</sup> The ETF approximation treats exchange and correlation effects in a local density approximation. On the other hand, it includes the von Weizsäcker quantum correction to the kinetic energy

$$T_W = \frac{\beta}{8} \int \frac{(\nabla n)^2}{n} d\vec{r}, \quad (2)$$

in addition to the local Thomas-Fermi term. We have used an effective value  $\beta=0.5$  [in Hartree atomic units (a.u.)] for the coefficient of the von Weizsäcker correction.<sup>20</sup> The semiclassical ETF method cannot account for shell effects, which should be included in any proper study of small alkali-metal clusters in order to predict the most probable fission channel among all the possible  $p$  values [see (1)]. However, for a fixed decay channel, the ETF method gives the correct value of the fusion barrier height  $B_m$ , i.e., the barrier height referred to the energy of the fragments at infinite separation. This has been explicitly shown in the case considered here, namely  $\text{Na}_{42}^{2+} \rightarrow 2 \text{Na}_{21}^+$ , by performing a fully self-consistent Kohn-Sham (KS) calculation within the TJS model,<sup>21</sup> and it supports the use of the ETF approximation to calculate  $B_m$  for that reaction. The fission-barrier height can then be obtained from the relationship

$$F_m = \Delta H_f + B_m, \quad (3)$$

where  $\Delta H_f$  is the heat of fission

$$\Delta H_f = 2E(\text{Na}_{21}^+) - E(\text{Na}_{42}^{2+}), \quad (4)$$

that is, the difference between the energy of the fragments at infinite separation and that of the spherical parent cluster.

Figure 1 displays the evolution of the total energy as a function of fragment separation when the fission path is described by means of intersecting jellium spheres ( $\lambda = 1 - \rho$ ). Plotted at the bottom of the figure are snapshots of the positive background along the fission path at the corresponding  $s$  values. The dotted vertical line at  $s = 22$  a.u. indicates the scission separation (touching jellium spheres in this case), i.e., the starting point in the TJS model. For  $s > 22$  a.u. the jellium configurations correspond to two separated spheres ( $\lambda = 0, \rho > 1$ ) and we recover the results of the previous TJS model. The  $1/s$  curve (dashed line) is the classical Coulomb repulsion between the fragments as point charges and the horizontal line in the right side corresponds to the energy of the final state. The maximum of the barrier occurs at  $s \simeq 30$  a.u. and the fission-barrier height has a value of 3.17 eV (0.85 eV for the fusion barrier height).

Figure 2 shows the barrier obtained for a different pathway parametrization in which the fissioning cluster forms a neck at  $s \simeq 20$  a.u. The scission distance is larger than in the previous case, but we obtain the same values as before for the barrier height and for the position

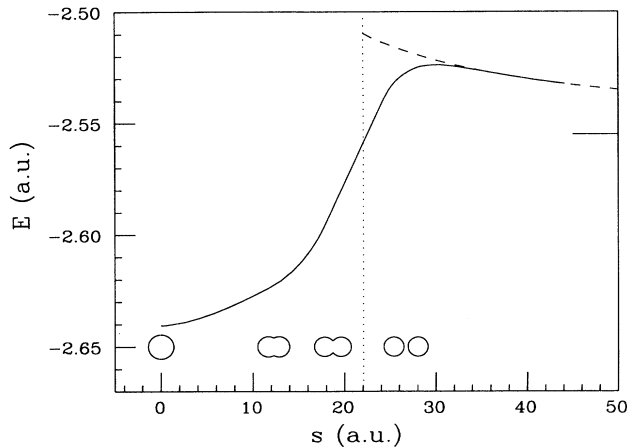


FIG. 1. ETF fission barrier for  $\text{Na}_{42}^{2+} \rightarrow 2 \text{Na}_{21}^+$  obtained when the fission pathway is described by intersecting jellium spheres up to the scission configuration (dotted line) and by two separated jellium spheres from this point on. The dashed line represents the classical Coulomb barrier and the horizontal line at the right side corresponds to the energy of the final state.

of the maximum. In the fission path corresponding to Fig. 3, the neck variation is slower than in the previous cases. This leads to a larger barrier height and scission occurs for a separation greater than the position of the maximum of the barrier. Within our model, the value of the fission-barrier height corresponds to the lowest result obtained (Figs. 1 or 2).

The calculations shown in Figs. 1–3 constitute the key result of this study, which can be summarized as follows: within the jellium model, the saddle configuration corresponds to two disconnected, spherical in the present case, jellium pieces tied up by the electronic cloud. We would like to stress that this holds even in the study of symmetric fission, in which two large clusters are emerging. The conclusion would not be modified if a KS instead of a ETF calculation is carried out, since the maximum of

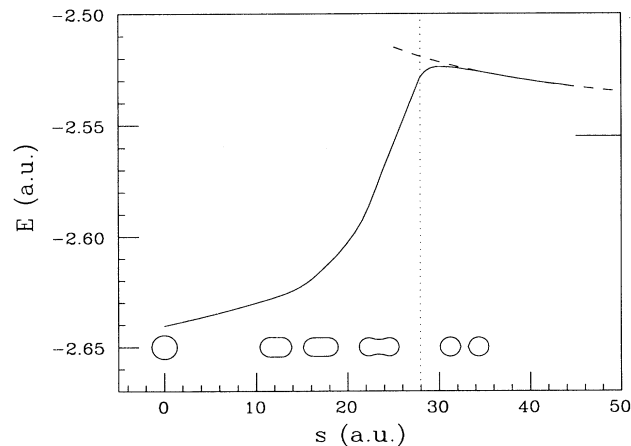


FIG. 2. Same as Fig. 1 using elongated jellium configurations and imposing the fastest variation of the neck.

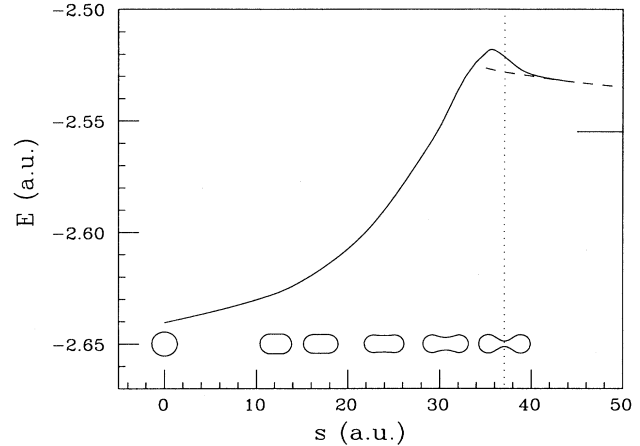


FIG. 3. Same as Fig. 2 for a slower variation of the neck.

the barrier occurs when the two jellium pieces are well apart, and humps and other structures originated by shell effects are found at much shorter distances.<sup>16,25</sup> As a final comment, the chief importance of self-consistently incorporating the electronic spillout to describe such extended saddle configurations should not be overlooked.

As a second example, we have also considered the asymmetric fission  $\text{Na}_{24}^{2+} \rightarrow \text{Na}_{21}^+ + \text{Na}_3^+$ , whose ETF fission barrier is shown in Fig. 4. The solid line has been obtained using the decaying path corresponding to the jellium configurations schematically shown at the bottom of this figure. Scission occurs at  $s \approx 23$  a.u. The dashed line corresponds to the intersecting-jellium-sphere fission path, as in Ref. 26 (similar to that of Fig. 1 although in the present case the jellium spheres have different sizes), with the scission point at  $s \approx 17$  a.u. (the jellium configuration shown at the top). Also for this asymmetric case

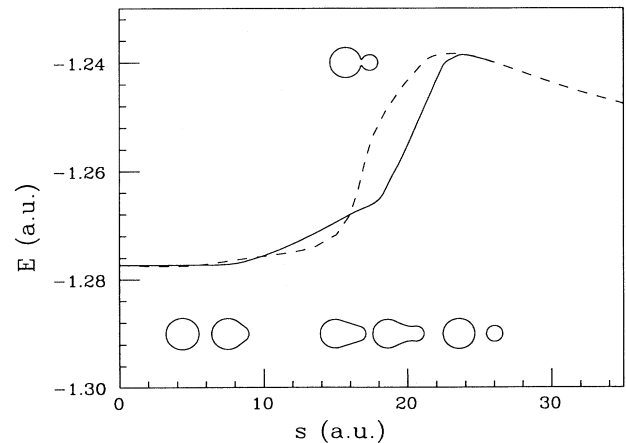


FIG. 4. ETF fission barrier for  $\text{Na}_{24}^{2+} \rightarrow \text{Na}_{21}^+ + \text{Na}_3^+$ . The solid line corresponds to the fission pathway described by the jellium configurations schematically shown at the bottom, whose scission point occurs at  $s \approx 23$  a.u. The dashed line is the result for intersecting jellium spheres, similar to Fig. 1 (scission occurs at  $s \approx 17$  a.u., upper jellium configuration).

we verify that the simple TJS model yields the same fission barrier height as the DJ model,  $F_m = 1.05$  eV, with the position of the maximum at  $s \simeq 24$  a.u. (the fission barrier height  $B_m$  is, in this case, equal to 1.03 eV). We conclude again that the maximum of the fission barrier corresponds to a configuration in which the emerging singly charged fragments are already formed and slightly tied up by the electron cloud. Thus, if the goal is the calculation of the barrier height and not the detailed shape of the barrier itself, one can obtain the correct results for the barrier height from the simpler model of two perfect jellium spheres with increasing separation between their centers (starting at the touching configuration).

The TJS model has already been used within the ETF method to calculate the critical value for the competition between neutral monomer evaporation and the most asymmetric fission in  $\text{Na}_N^{2+}$  clusters, which turned out to be  $N_c = 36$ , in qualitative agreement with the experimental result  $N_c = 27$ . Consideration of other fission channels, like  $\text{Na}_3^+$  emission,<sup>20</sup> leads to a decrease of the critical number. The predicted critical size for spontaneous fission of  $\text{Na}_N^{2+}$  clusters is  $N_c^* \simeq 10$ . Another interesting result obtained for the fission of  $\text{Na}_N^{2+}$  is that the height of the ETF fission barrier can be estimated from the classical Coulomb repulsion between the two fragments, considered as point charges, and separated by a distance such that their electron densities begin to overlap.<sup>15,22</sup>

Since for large clusters shell effects tend to play a diminishing role, the semiclassical extended Thomas-Fermi model is expected to exhibit the main trends of excited medium-size or large cluster fragmentation. This is indeed the case for highly charged alkali-metal clusters  $M_N^{q+}$ , for which it is reasonable to assume that charged trimer emission is the predominant fission channel. The comparison between ETF and pure Coulomb barriers further suggests a simple approximation for the fission-barrier height:

$$F_m = \Delta H_f + \frac{q-1}{r_s[(N-3)^{1/3} + 3^{1/3}] + D_3}, \quad (5)$$

where  $r_s$  is the Wigner-Seitz radius of the metal and  $D_3$  is an effective distance that serves to take care of the large electron spillout beyond the jellium edge. We have verified that the experimental critical sizes for  $\text{Na}_N^{q+}$  clusters with  $q > 2$  are well reproduced by simple spherical extended Thomas-Fermi calculations in which one compares the heat of monomer evaporation with the fission barrier obtained from Eq. (5) using an effective value  $D_3 = 18$  a.u. (see Table I). Note that  $D_3$  gives, on average, the separation between the TJS contact configuration and the point at which the pure Coulomb bar-

TABLE I. Critical numbers for the competition between neutral monomer evaporation and charged trimer emission in  $\text{Na}_N^{q+}$  clusters, as obtained using Eq. (5) with  $D_3 = 18$  a.u., in comparison with experimental values (Ref. 3). Last column corresponds to the absolute critical sizes for spontaneous fission in the same approximation.

$q$	$N_c$	$N_c$ (expt.)	$N_c^*$
3	66	$63 \pm 1$	28
4	126	$123 \pm 2$	56
5	207	$206 \pm 4$	95
6	305	$310 \pm 10$	140
7	420	$445 \pm 10$	195

rier equals the ETF barrier maximum. One should avoid confusion with the so-called “spillout parameter” in the literature.

Although more complicated, the model presented in this paper can be extended to study multifragmentation of clusters with  $q \geq 3$ . However, we did not consider this possibility since no evidence for multifragmentation exists in the literature.

We stress again that the ETF energy functional is unable to account for electronic shell effects, which determine in many cases the nature of the preferred fission channels, and a full Kohn-Sham calculation of the fission barriers for the different possible channels is desirable (this calculation has already been performed for selected channels in the TJS model<sup>21</sup>). Nevertheless, with reference to Eq. (3), giving the fission-barrier height as a sum of two terms, those shell effects have a strong influence on the values of the heat of fission  $\Delta H_f$  (final state effect) but a relatively minor effect on  $B_m$ . This fact suggests the calculation of  $F_m$  by combining the ETF fusion barriers with the heats of fission obtained from Kohn-Sham calculations, which are easy to perform for the undeformed parent and for fragments infinitely separated. This should provide a fair approximation to  $F_m$ .

In summary, in this paper we have calculated the barriers for fission of multiply charged clusters using a deformed-jellium model. As the main result we have found that the saddle configuration corresponds to two disconnected jellium pieces tied up by the electronic cloud.

## ACKNOWLEDGMENTS

This work has been partially supported by the DG-ICYT (Spain), Grant Nos. PB92-0021-C02-02, PB92-0645-C03-01, and PB92-0761, and by Caja Cantabria.

<sup>1</sup> K. Sattler, J. Mühlbach, O. Echt, P. Pfau, and E. Recknagel, Phys. Rev. Lett. **47**, 160 (1981).

<sup>2</sup> T. P. Martin, U. Näher, H. Göhlich, and T. Lange, Chem. Phys. Lett. **196**, 113 (1992).

<sup>3</sup> U. Näher, S. Frank, N. Malinowski, U. Zimmermann, and T. P. Martin, Z. Phys. D **31**, 191 (1994).

<sup>4</sup> C. Bréchnignac, Ph. Cahuzac, F. Carlier, and M. de Frutos, Phys. Rev. Lett. **64**, 2893 (1990).

- <sup>5</sup> C. Bréchnignac, Ph. Cahuzac, F. Carlier, J. Leygnier, and A. Sarfati, *Phys. Rev. B* **44**, 11 386 (1991); C. Bréchnignac, Ph. Cahuzac, F. Carlier, and M. de Frutos, *ibid.* **49**, 2825 (1994).
- <sup>6</sup> P. Pfau, K. Sattler, R. Pflaum, and E. Recknagel, *Phys. Lett.* **104A**, 262 (1984).
- <sup>7</sup> D. Tomanek, S. Mukerjee, and K. H. Bennemann, *Phys. Rev. B* **28**, 665 (1983).
- <sup>8</sup> B. K. Rao, P. Jena, M. Manninen, and R. M. Mieminen, *Phys. Rev. Lett.* **58**, 1188 (1987).
- <sup>9</sup> C. Baladrón, J. M. López, M. P. Iñiguez, and J. A. Alonso, *Z. Phys. D* **11**, 323 (1989).
- <sup>10</sup> F. Liu, M. R. Press, S. N. Khanna, and P. Jena, *Phys. Rev. Lett.* **59**, 2562 (1987).
- <sup>11</sup> F. Reuse, S. N. Khanna, V. de Coulon, and J. Buttet, *Phys. Rev. B* **41**, 11 743 (1990).
- <sup>12</sup> W. A. Saunders, *Phys. Rev. Lett.* **64**, 3046 (1990); **66**, 840 (1991); *Phys. Rev. A* **46**, 7028 (1992).
- <sup>13</sup> E. Lipparini and A. Vitturi, *Z. Phys. D* **17**, 57 (1990).
- <sup>14</sup> M. Nakamura, Y. Ishii, A. Tamura, and S. Sugano, *Phys. Rev. A* **42**, 2267 (1990).
- <sup>15</sup> F. Garcias, J. A. Alonso, J. M. López, and M. Barranco, *Phys. Rev. B* **43**, 9459 (1991); J. A. Alonso, J. M. López, C. Baladrón, F. Garcias, and M. Barranco, *An. Fís. A* **87**, 131 (1991); M. Barranco, J. A. Alonso, F. Garcias, and J. M. López, in *Clustering Phenomena in Atoms and Nuclei*, edited by M. Brenner, T. Lönnroth, and F. B. Malik (Springer, New York, 1992), p. 305.
- <sup>16</sup> R. N. Barnett, U. Landman, and G. Rajagopal, *Phys. Rev. Lett.* **67**, 3058 (1991); C. Bréchnignac, Ph. Carlier, M. de Frutos, R. N. Barnett, and U. Landman, *ibid.* **72**, 1636 (1994).
- <sup>17</sup> V. Strutinsky, *Nucl. Phys.* **A95**, 420 (1967); **122**, 1 (1968); M. Brack, J. Damgaard, A. S. Jensen, H. C. Pauli, V. M. Strutinsky, and C. Y. Wong, *Rev. Mod. Phys.* **44**, 320 (1972).
- <sup>18</sup> H. Koizumi, S. Sugano, and Y. Ishii, *Z. Phys. D* **26**, 264 (1993); **28**, 223 (1993).
- <sup>19</sup> P. Hohenberg and W. Kohn, *Phys. Rev.* **136**, B864 (1964).
- <sup>20</sup> J. M. López, J. A. Alonso, F. Garcias, and M. Barranco, *Ann. Phys. (Leipzig)* **1**, 270 (1992).
- <sup>21</sup> J. A. Alonso, M. Barranco, F. Garcias, and J. M. López, *Comments At. Mol. Phys.* (to be published); F. Garcias, J. A. Alonso, M. Barranco, J. M. López, A. Mañanes, and J. Németh, *Z. Phys. D* **31**, 275 (1994).
- <sup>22</sup> J. M. López, J. A. Alonso, N. H. March, F. Garcias, and M. Barranco, *Phys. Rev. B* **49**, 5565 (1994).
- <sup>23</sup> J. Blocki, *J. Phys. (Paris) Colloq.* **45**, C6-489 (1984); J. Blocki, R. Planeta, J. Brzychczyk, and K. Grotowski, *Z. Phys. A* **341**, 307 (1992).
- <sup>24</sup> R. Beringer, *Phys. Rev.* **131**, 1402 (1963).
- <sup>25</sup> E. Engel, U. R. Schmitt, H.-J. Lüdde, A. Toepfer, E. Wüst, R. M. Dreizler, O. Knospe, R. Schmidt, and P. Chattopadhyay, *Phys. Rev. B* **48**, 1862 (1993).
- <sup>26</sup> S. Saito and M. L. Cohen, *Phys. Rev. B* **38**, 1123 (1988).